Oil and Protein Accumulation in Developing Seeds Is Influenced by the Expression of a Cytosolic Pyrophosphatase in Arabidopsis[C][W][OA]

Knut Meyer*, Kevin L. Stecca, Kim Ewell-Hicks, Stephen M. Allen, and John D. Everard

Pioneer, A DuPont Company, Agricultural Biotechnology, Wilmington, Delaware 19880

This study describes a dominant low-seed-oil mutant (lo15571) of Arabidopsis (*Arabidopsis thaliana*) generated by enhancer tagging. Compositional analysis of developing siliques and mature seeds indicated reduced conversion of photoassimilates to oil. Immunoblot analysis revealed increased levels of At1g01050 protein in developing siliques of lo15571. At1g01050 encodes a soluble, cytosolic pyrophosphatase and is one of five closely related genes that share predicted cytosolic localization and at least 70% amino acid sequence identity. Expression of At1g01050 using a seed-preferred promoter recreated most features of the lo15571 seed phenotype, including low seed oil content and increased levels of transient starch and soluble sugars in developing siliques. Seed-preferred RNA interference-mediated silencing of At1g01050 and At3g53620, a second cytosolic pyrophosphatase gene that shows expression during seed filling, led to a heritable oil increase of 1% to 4%, mostly at the expense of seed storage protein. These results are consistent with a scenario in which the rate of mobilization of sucrose, for precursor supply of seed storage lipid biosynthesis by cytosolic glycolysis, is strongly influenced by the expression of endogenous pyrophosphatase enzymes. This emphasizes the central role of pyrophosphate-dependent reactions supporting cytosolic glycolysis during seed maturation when ATP supply is low, presumably due to hypoxic conditions. This route is the major route providing precursors for seed oil biosynthesis. ATP-dependent reactions at the entry point of glycolysis in the cytosol or plastid cannot fully compensate for the loss of oil content observed in transgenic events with increased expression of cytosolic pyrophosphatase enzyme in the cytosol. These findings shed new light on the dynamic properties of cytosolic pyrophosphate pools in developing seed and their influence on carbon partitioning during seed filling. Finally, our work uniquely demonstrates that genes encoding cytosolic pyrophosphatase enzymes provide novel targets to improve seed composition for plant biotechnology applications.

During the maturation phase of seed development, photoassimilates, mainly Suc and amino acids, are converted to the seed storage compounds starch, seed storage lipids, and proteins (Ruan and Chourey, 2006; Baud et al., 2008; Meyer and Kinney, 2010). A complete understanding of the properties of this pathway, specifically the control points influencing the partitioning of carbon between starch, oil, and protein, has been the focus of diverse research approaches due to the importance of seed storage compounds in human civilization as sources of food, feed, and fuel.

In a developing cruciferous oil seed, such as Arabidopsis (*Arabidopsis thaliana*), factors controlling carbon partitioning have been identified through analysis of recessive mutants with altered oil content. Characterization of a recessive high-oil mutant has led to the identification of maternally controlled deposition polysaccharides of the seed coat mucilage as a carbon sink that diverts carbon from seed storage lipid biosynthesis (Shen et al., 2006; Shi et al., 2012). Transfer (T)-DNA-tagged alleles of plastidic subunits of pyruvate kinase are associated with low seed oil content and have demonstrated the importance of plastidic pyruvate supply in seed storage lipid biosynthesis (Andre et al., 2007; Baud et al., 2007b). Defects in plastidic starch biosynthesis, due to recessive loss-of-function mutations of plastidic phosphoglucomutase, show low seed oil content, thus emphasizing the importance of transient starch as a carbon source supporting seed oil biosynthesis in Arabidopsis (Periappuram et al., 2000). Characterization of a recessive mutant, *wrinkled1* (*wri1*), with low oil and increased accumulation of soluble sugars and starch led to the identification of a class of global transcriptional regulators of glycolysis and early reactions of plastidic fatty acid biosynthesis that respond to developmental cues provided by regulators of embryo development, such as *LEAFY COTYLEDON1* (*LEC1*), *LEC2*, *FUSCA3*, and *ABSCISIC ACID INSENSITIVE3* (Focks and Benning, 1998; Cernac and Benning, 2004; Baud et al., 2007a; Santos-Mendoza et al., 2008).

Additional factors controlling carbon partitioning during seed fill have been identified by transcriptome analysis. This analysis is most powerful when applied

* Corresponding author; e-mail knut.meyer@usa.dupont.com.

The author responsible for distribution of materials integral to the findings presented in this article in accordance with the policy described in the Instructions for Authors (www.plantphysiol.org) is: Knut Meyer (knut.meyer@usa.dupont.com).

[C] Some figures in this article are displayed in color online but in black and white in the print edition.

[W] The online version of this article contains Web-only data.

[OA] Open Access articles can be viewed online without a subscription.

www.plantphysiol.org/cgi/doi/10.1104/pp.112.198309

to mutants or to closely related germplasm with great differences in seed composition (Bourgis et al., 2011) or divergent oil seed species (Troncoso-Ponce et al., 2011). For example, the comparative analysis of the *wri1* mutant and wild-type Arabidopsis seed has demonstrated that genes controlling cytosolic reactions of early glycolysis (Suc synthase, hexokinase, pyrophosphate-dependent phosphofructokinase [PFP]) and plastidic reactions of later steps of glycolysis (pyruvate kinase) are regulated by the WRI1 gene product (Ruuska et al., 2002). This observation was later confirmed by in situ visualization of said enzyme activities in developing Arabidopsis embryos (Baud and Graham, 2006).

Finally, a global picture of reactions supporting storage compound metabolism and their relative importance in developing seed can be derived from metabolic flux analysis (MFA; Schwender, 2008, 2011; Allen et al., 2009a). MFA analysis demonstrated that increased carbon efficiency in the developing, green seeds of the Brassicaceae is due to a modification of plastidic glycolysis. CO_2 released by the plastidic pyruvate dehydrogenase complex is captured by Rubisco-mediated synthesis of phosphoglycerate, thus bypassing the glyceraldehyde-3-phosphate dehydrogenase and phosphoglycerate kinase reactions of traditional glycolysis (Ruuska et al., 2004; Schwender et al., 2004). More recently, MFA of developing soybean (*Glycine max*) seed and maize (*Zea mays*) embryos highlights the importance of plastidic malic enzyme generating pyruvate and NADPH reductant for plastidic fatty acid biosynthesis (Allen et al., 2009b; Alonso et al., 2010).

Our rapidly increasing understanding of the network of reactions that support anabolic pathways leading to oil, protein, and starch biosynthesis in developing seed is currently not reflected in the sophistication of transgenic approaches targeting the biotechnological modification of carbon partitioning in seed. For example, most transgenic approaches to increase the oil content of seed are composed either of attempts to increase "pull" toward oil biosynthesis through the increased expression of genes controlling plastidic fatty acid biosynthesis or cytosolic glycerolipid assembly (Roesler et al., 1997; Zou et al., 1997; Jako et al., 2001; Vigeolas et al., 2007; Zheng et al., 2008) or by increasing metabolic "push" in this direction through the overexpression of developmental or global metabolic regulators that enhance the expression of genes encoding enzymes of glycolysis and fatty acid biosynthesis (Shen et al., 2010; Pouvreau et al., 2011; Tan et al., 2011). Notable exceptions include the seed-specific expression of class 2 hemoglobins to address oxygen-limiting conditions during the seed maturation phase (Vigeolas et al., 2011).

This contribution describes an approach that employs methods, complementary to those described above, to greatly increase the number of gene targets affecting carbon partitioning in developing seed. Our goal was the identification of components of the seed-filling machinery that divert carbon away from the accumulation of seed storage lipids, thus providing new gene targets for increasing the oil content of plant tissues through RNA interference (RNAi)-mediated down-regulation. To this end, we screened enhancer tag libraries of Arabidopsis for dominant low-oil mutants. We used this approach because low oil content (increased seed density) is a phenotype amenable to low-cost, high-throughput screening using density gradients. Here, we describe the detailed characterization of one of these mutants, the molecular identification of the gene responsible for the low-oil phenotype and the utility of the identified gene target to increase the oil content of plant tissues. Our results highlight the importance of soluble, cytosolic pyrophosphatase activity in determining the glycolytic conversion of photoassimilates to precursors of seed storage lipid.

RESULTS

Identification and Characterization of a Dominant Low-Seed-Oil Mutant of Arabidopsis

A library of Arabidopsis enhancer tag mutants was previously generated with pHSbarENDsII, providing a quadruple 35S enhancer sequence in the proximity of the right T-DNA border (Supplemental Fig. S1; H. Sakai, unpublished data). T3 seed pools, derived from grow-outs of T2 lines, of 96 events were subjected to density gradient screening (Focks and Benning, 1998). High-density seed were recovered and plated on selective medium. Seedlings were transferred to soil and grown to maturity alongside untransformed control plants. Seed oil content was determined nondestructively by ^{1}H-NMR. In this manner, a total 520 T3 seed pools, derived from approximately 50,000 independent enhancer tag insertion lines, were screened.

A mutant line, lo15571, showed a heritable oil decrease of 5% relative to wild-type seed (Fig. 1, A and B). No segregants could be recovered that were homozygous for the transgene conferring phosphinothricin resistance, indicating that a gene that is essential for embryo development was disrupted by the transgene insertion in lo15571. T5 plants were back-crossed to Arabidopsis wild-type plants. Pollen of lo15571 plants was used to fertilize emasculated, immature flowers of wild-type plants. F1 seed were germinated on medium containing phosphinothricin. Herbicide-tolerant F1 and F2 seedlings were grown to maturity. Twenty-four herbicide-resistant progeny derived from a F2 plant heterozygous for the transgene conferring phosphinothricin resistance were planted in the same flat alongside six wild-type and lo15571 mutant plants. The seed oil content of all 24 progeny was uniformly low, namely indistinguishable from the lo15571 mutant parent (Fig. 1C). This suggests that the transgene insertion associated with phosphinothricin herbicide tolerance confers a dominant low-oil phenotype.

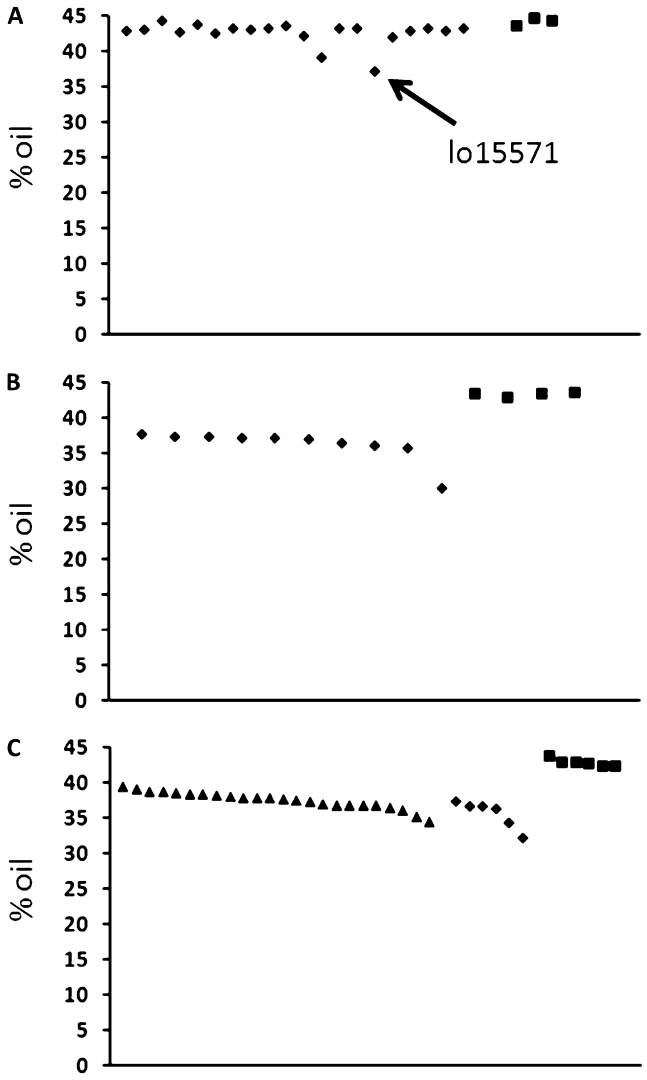

Figure 1. A, Seed oil content of T3 plants derived from low-oil (high-density) seed selected by density gradient centrifugation of T3 seed pool 225 representing 96 independent pHSbarENDs2 events (diamonds) and untransformed wild-type control plants (squares). B, Seed oil content of phosphinothricin-resistant T4 progeny of lo15571 (diamonds) and untransformed wild-type control plants (squares). C, Seed oil content of phosphinothricin-resistant BC0F2 progeny of a plant that was heterozygous for the lo15571 transgene (triangles), phosphinothricin-resistant T6 progeny of the lo15571 parent (diamonds), and untransformed wild-type control plants (squares).

Twenty-four herbicide-tolerant F4 progeny of the back-crossed lo15571 mutant were grown in the same flat alongside 12 plants of the untransformed Arabidopsis parent. Silique tissue was bulk harvested, by type, 28 d after transfer to soil. Plants from a second flat planted in a similar fashion were grown to maturity, and dry seeds were bulk harvested by type. Silique and seed tissues were subjected to quantitative analysis of oil, protein, soluble sugars, and starch.

The presence of the lo15571 transgene leads to an overall shift in the composition of both developing siliques and mature seed that is characterized by increased soluble carbohydrate and starch and reduced levels of seed storage compounds. In developing siliques, this shift is characterized by increased levels of Fru, Glc, Suc, and starch and a reduction in protein (Table I). In dry seeds, the lo15571-related shift results in increased levels of Fru and Glc and a reduction of seed storage lipid (Table II). The lo15571 mutant shows a small increase in seed size that has also been observed in other Arabidopsis mutants with altered carbon partitioning in developing seed (Periappuram et al., 2000, Chen and Thelen, 2011). In summary, the observations suggest that a reduced conversion of photoassimilate to seed storage compounds is the basis for the dominant low-oil phenotype of the lo15571 enhancer tag line.

Candidate Gene Identification: Identification of an Enhancer Tag Insertion That Leads to Altered Expression of At1g01050

Genomic DNA was extracted from leaf material of T5 plants of lo15571. Genomic DNA sequence flanking the T-DNA insert in the lo15571 mutant line was cloned and sequenced using selected amplification of insertion flanking fragments (SAIFF; Muszynski et al., 2006). A single amplified fragment was identified containing the T-DNA border sequence and Arabidopsis genomic sequence. Once the genomic sequence flanking a T-DNA insert was obtained, a genomic region of interest was identified by alignment to the completed Arabidopsis genome sequence at The Arabidopsis Information Resource 10 (http://www.arabidopsis.org/servlets/sv). Specifically, the SAIFF PCR product generated with PCR primers corresponding to the left border sequence of the T-DNA present in pHSbarENDs2 (Supplemental Fig. S1) aligns with nucleotides 1,221 to 1,541 of the Arabidopsis gene At1g01040. The gene is also known as DICER-Like1 (DCL1), and mutant alleles of this gene such as *carpel factory*, *suspensor1*, *short integument1*, *abnormal suspensor1*, *emb76*, and *emb60* have been characterized (Schauer et al., 2002). The gene is annotated as an ATP-dependent helicase/RNaseIII with strong sequence similarity to the DICER class of proteins, which act in microRNA processing. The DNA sequence generated using SAIFF and genomic DNA of lo15571 matches sequence of the first and second exons and first intron of At1g01040. Because of the location of the T-DNA in lo15571, we conclude that, like the *emb60* and *emb70* alleles of DCL1 (Schauer et al., 2002), the T-DNA insertion allele of DCL1 present in lo15571 encodes a nonfunctional product of said gene that leads to embryo lethality in segregants homozygous for the lo15571 transgene. The uniformly low-seed-oil phenotype of all herbicide-resistant F3 plants derived from an F2 plant heterozygous for the lo15571 transgene illustrated in Figure 1C suggests that the disruption of At1g01040 is not related to the low-seed-oil phenotype of lo15571.

The gene At1g01050 is approximately 9 kb upstream of the sequence adjacent to the left T-DNA border in

Table I. *Composition of developing siliques of the lo15571 enhancer tag mutant and untransformed wild-type control plants*

Twenty-four lo15571 plants were grown in the same 36-cell flat alongside 12 wild-type plants. Silique tissue was bulk harvested by type 28 d after planting, homogenized, and lyophilized. Oil content was measured gravimetrically. Protein content was measured by combustion analysis. Soluble carbohydrate composition was determined by gas chromatography analysis of derivatized oligomeric or monomeric sugars. Starch content was measured by digestion of the insoluble residue with a mixture of starch hydrolases followed by gas chromatography-based quantitation of derivatized Glc. Analyses were performed in triplicate. Mean comparisons that were not significant at the 10% level (probT, homoscedastic *t* test ≤ 0.1; Microsoft Excel) are indicated by ns.

Plant	Value	Fru	Glc	Suc	Galactinol + Raffinosaccharides	Total Soluble Sugars	Starch	Protein	Oil	Protein + Oil	Soluble Sugars + Starch
lo15571	Mean	0.48	1.74	1.62	0.08	3.9	3.6	24.6	11.7	36.3	7.5
	SD	0.04	0.13	0.05	0.02	0.2	0.1	0.8	0.5		
Wild type	Mean	0.19	0.87	1.09	0.05	2.2	2.3	27.3	11.8	39.1	4.5
	SD	0.01	0.03	0.06	0.00	0.1	0.3	1.7	0.1		
	Percentage change	154	101	49	68	79	56	−10	−1 (ns)	−7	68

lo15571. This gene is annotated as cytosolic, soluble pyrophosphatase (PPiase); it is also known as PPA1. Cytosolic localization of the gene product has been confirmed by microscopic visualization of At1g01050-GFP fusion proteins in transgenic plants (Koroleva et al., 2005). Heterologous expression of PPA1 in *Escherichia coli* and in-depth characterization of enzyme activity demonstrate that this enzyme is a monomeric, Mg^{2+}-dependent phosphatase that is strictly specific to the pyrophosphate substrate (Navarro-De la Sancha et al., 2007).

To test if altered expression of At1g01050 is associated with the altered seed composition of the lo15571 mutant, immunological tools for At1g01050 detection were developed. The At1g01050 protein was recombinantly produced in *E. coli*. The open reading frame (ORF) was cloned into pET29a, creating an in-frame fusion with a C-terminal hexa-His tag. C-terminally His-tagged At1g01050 was purified from *E. coli* cultures using Ni^{2+} affinity chromatography and used to raise polyclonal antisera in rabbits. The resulting antiserum has a detection limit below 5 ng of the recombinantly produced At1g01050 protein (Fig. 2). Total protein was extracted from the developing silique tissue used previously for compositional analysis (Table I) and subjected to western analysis. Silique protein extracts of lo15571 show increased abundance of a protein of approximately 25 kD that is detected by the polyclonal antiserum raised against the purified At1g01050 gene product (Fig. 2). This supports the notion that increased PPiase enzyme expression is causing reduced seed oil accumulation in the lo15571 mutant.

Gene Validation: Characterization of Transgenic Events with Seed-Preferred Overexpression of At1g01050

To further test this hypothesis and to clarify the extent to which increased PPiase expression in developing seed, specifically during the seed maturation phase, affects seed storage compound accumulation, the At1g01050 ORF was expressed under the control of a strong seed-preferred promoter. To this end, the At1g01050 gene was fused to the soybean Glycinin1 (GY1) promoter. The soybean GY1 seed storage protein promoter is derived from soybean gene Glyma03g32030.1 and is known to confer strong seed-preferred gene expression in transgenic applications (Nielsen et al., 1989; Iida et al., 1995). A total of 18 transgenic events were generated with the binary vector pKR1478-PPA1 (Supplemental Fig. S2). T1

Table II. *Composition of mature seeds of the lo15571 enhancer tag mutant and untransformed wild-type control plants*

Twenty-four lo15571 plants were grown in the same 36-cell flat alongside 12 wild-type plants. Seeds were bulk harvested by type, homogenized, and analyzed as described for Table I. Percentage weight values are given at 5% moisture. Mean comparisons that were not significant at the 10% level (probT, homoscedastic *t* test ≤ 0.1; Microsoft Excel) are indicated by ns.

Plant	Value	Fru	Glc	Suc	Galactinol + Raffinosaccharides	Total Soluble Sugars	Starch	Protein	Oil	Protein + Oil	Soluble Sugars + Starch	Seed Weight
												μg
lo15571	Mean	0.34	1.27	1.96	0.66	4.2	0.066	22.5	35.0	57.5	4.3	23.8
	SD	0.01	0.03	0.01	0.04	0.1	0.019	1.2	0.5	1.6		0.2
Wild type	Mean	0.04	0.84	1.81	0.65	3.3	0.028	21.7	39.3	60.9	3.4	20.6
	SD	0.01	0.03	0.07	0.07	0.1	0.006	2.7	1.5	2.6		0.5
	Percentage change	685	52	8	1 (ns)	27	133	4 (ns)	−11	−14 (ns)	27	16

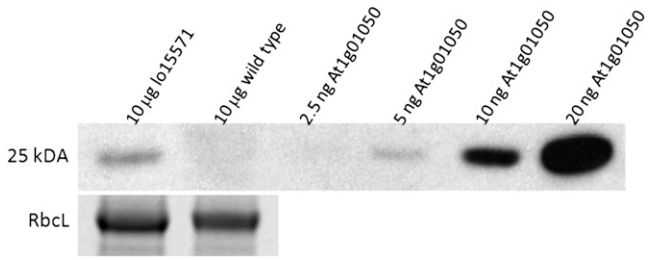

Figure 2. Immunoblot analysis of At1g01050 protein expression in developing siliques of the lo15571 enhancer tag mutant and wild-type Arabidopsis plants. Buffer-exchanged silique protein extracts and recombinantly produced At1g01050 protein standards were separated by SDS-PAGE and transferred to a nitrocellulose membrane. The At1g01050 protein was detected with polyclonal rabbit antisera raised against the purified At1g01050 protein. A second SDS-PAGE gel was run with identical samples. The Coomassie Blue-stained large subunit of Rubisco (RbcL) is provided as a loading control for the silique protein samples.

plants from nine independent events were grown alongside six untransformed control plants. Seeds were bulk harvested from mature wild-type plants or harvested and analyzed individually in case of transgenic events. Oil content was measured by ^{1}H-NMR. The great majority of events generated with a construct for seed-preferred expression of At1g01050 show a reduction in seed oil content ranging between 3.1% and 13.8% when compared with wild-type plants grown in the same flat (Fig. 3A). Two events, K46562 and K46564, were allowed to self. Homozygous T3 seed from the K46562 and K46564 events showed a heritable reduction in oil content ranging between 5% and 8% when compared with wild-type Arabidopsis plants grown under identical conditions (Fig. 3, B and C).

Immunoblot analysis indicates increased levels of the At1g01050 protein in developing siliques of events K46562 and K46564 similar to lo15571 (Fig. 4). Homozygous T3 progeny of K46562 and K46564 were grown in the same flat alongside the untransformed Arabidopsis parent. Silique tissue was bulk harvested by type 28 d after transfer to soil. Plants in a second flat planted in a similar fashion were grown to maturity, and dry seeds were bulk-harvested by type. Developing silique tissue and mature seed were subjected to quantitative analysis of oil, protein soluble sugars, and starch, and the results are shown in Tables III and IV, respectively.

The presence of the GY1::At1g01050 transgene leads to an overall shift in the composition of both siliques and mature seed that is closely related to the compositional phenotype of the lo15571 enhancer tag line (Tables I and II). There are, however, slight differences between the two genotypes. Developing siliques of the GY1::At1g01050 events show an even greater reduction in protein and oil (Table III). The total increase of carbohydrate, including soluble and starch fractions, is similar when lo15571 and GY1::AT1g01050 events are compared; however, in the latter, there is a greater increase in starch and a smaller increase in soluble sugars (Table III). Differences between lo15571 and the GY1::At1g01050 events are even more apparent when the composition of dry seeds is compared (Table IV). There is no increase of Fru in dry seeds, and the overall increase in soluble sugars compared with lo15571 is again reduced in the GY1 events. While oil is greatly decreased, there is a more substantial increase in protein that is more pronounced in the K46564 event. Finally, there is a small reduction in seed weight of 10% in GY1:At1g01050 events that was not apparent in the lo15571 mutant lines.

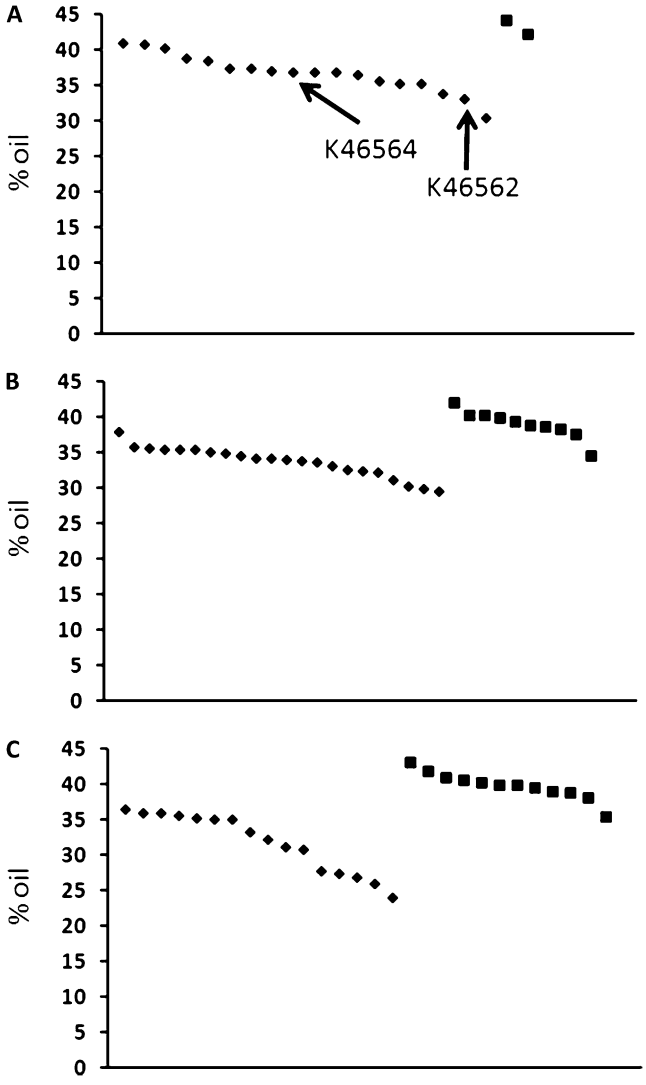

Figure 3. A, Seed oil content of T1 plants generated with a construct for expression of the At1g01050 gene under the control of the seed-preferred GY1 promoter (diamonds) and untransformed wild-type control plants (squares). B, Seed oil content of homozygous T3 plants of event K46564 (diamonds) and untransformed wild-type control plants (squares). C, Seed oil content of homozygous T3 plants of event K46562 (diamonds) and untransformed wild-type control plants (squares).

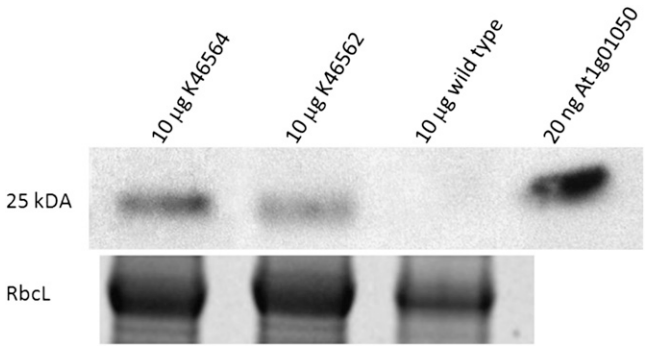

Figure 4. Immunoblot analysis of At1g01050 protein expression in developing siliques of wild-type plants and two homozygous transgenic events (K46562 and K46564) expressing At1g01050 under the control of the seed-preferred GY1 promoter. Buffer-exchanged silique protein extracts and a recombinantly produced At1g01050 protein standard were separated by SDS-PAGE and transferred to a nitrocellulose membrane. The At1g01050 protein was detected with polyclonal rabbit antisera raised against the purified At1g01050 protein. A second SDS-PAGE gel was run with identical samples. The Coomassie Blue-stained large subunit of Rubisco (RbcL) is provided as a loading control for the silique protein samples.

In summary, the fact that seed-preferred overexpression of At1g01050 almost perfectly recreates the lo15571 phenotype in developing siliques and dry seed provides a strong validation that the dominant, gain-of function, low-oil phenotype of the lo15571 mutant is caused by increased expression of a cytosolic pyrophosphatase enzyme, At1g01050. While the characterization of the lo15571 event alone, in particular the observation of increased At1g01050 protein levels in developing siliques, already strongly supports a connection between altered PPiase expression and the low-seed-oil phenotype, it does not clarify to which extent the seed phenotype is caused by alterations in carbohydrate metabolism in nonseed tissues, including source and other sink organs of the plant. This is due to the fact that At1g01050 is expressed during most stages of plant development (Navarro-De la Sancha et al., 2007) and that we do not know if and how patterns of At1g01050 expression are altered at the whole plant level due to the enhancer tag insertion. However, analysis of the GY1::At1g01050 events clarifies this and shows that increased At1g01050 protein abundance during the maturation phase of developing seed, most likely embryo tissues, leads to reduced conversion of sugars to seed storage lipid. Slight differences in seed composition between lo15571 and the GY1::At1g01050 events most likely can be attributed to differences in tissue specificity and the strength or timing of At1g01050 overexpression associated with the two transgenes.

Characterization of Transgenic Events with Seed-Preferred RNAi of Genes Encoding Cytosolic Pyrophosphatase Genes

Increased expression of cytosolic PPiase enzymes during the seed maturation phase impairs the mobilization of photoassimilates for oil and protein biosynthesis. This may be mediated through the depletion of cytosolic inorganic pyrophosphate (PPi), acting as substrate of the forward reaction of cytosolic enzymes such as UDP-glucose pyrophosphorylase (UGPase). This reaction is a central part of the Suc synthase pathway by which carbon enters the cytosolic hexose phosphate pool (Plaxton and Podesta, 2006). PPi is also substrate of the forward reaction of PFP at the entry point of glycolysis (Fig. 5; Plaxton, 1996).

Increased transient starch accumulation observed in developing siliques indicates that reduced flux through the forward reaction of UGPase alone is not responsible for the reduced oil accumulation. It is reasonable to assume that increased flux through invertase-mediated Suc mobilization and hexokinase-

Table III. *Composition of developing siliques of two events, K46562 and K46564, expressing At1g01050 under the control of the soybean GY1 promoter and untransformed wild-type control plants*

Twenty-four plants of K46562 or K46564 were grown in the same 36-cell flat alongside 12 wild-type plants. Silique tissue was bulk harvested by type 28 d after planting, homogenized, lyophilized, and analyzed as described for Table I. Percentage dry weight values are presented. Mean comparisons that were not significant at the 10% level (probT, homoscedastic *t* test ≤ 0.1; Microsoft Excel) are indicated by ns.

Plant	Value	Fru	Glc	Suc	Galactinol + Raffinosaccharides	Total Soluble Sugars	Starch	Protein	Oil	Protein + Oil	Soluble Sugars + Starch
K46564	Mean	0.42	1.65	2.10	0.44	4.7	6.2	19.5	11.8	31.3	10.9
	SD	0.04	0.11	0.14	0.08	0.3	0.6	0.6	0.5		
Wild type	Mean	0.23	1.25	2.22	0.43	4.1	2.8	21.6	14.6	36.2	6.9
	SD	0.08	0.08	0.11	0.05	0.0	0.2	0.7	0.8		
	Percentage change	85	32	−5 (ns)	2 (ns)	12	126	−10	−19	−14	58
K46562	Mean	0.66	1.89	2.66	0.12	5.3	10.2	16.0	10.7	26.7	15.5
	SD	0.03	0.08	0.17	0.01	0.1	0.0	0.7	0.0		
Wild type	Mean	0.35	1.30	2.02	0.08	3.8	5.6	21.9	11.6	33.5	9.3
	SD	0.02	0.12	0.03	0.01	0.2	0.3	0.5	0.6		
	Percentage change	88	45	32	32	42	82	−27	−8 (ns)	−20	66

Table IV. *Composition of mature seeds of two events, K46562 and K46564, expressing At1g01050 under the control of the soybean GY1 promoter and seed of untransformed wild-type control plants*

Twenty-four plants of K46562 or K46564 were grown in the same 36-cell flat alongside 12 wild-type plants. Seeds were bulk harvested by type, homogenized, and analyzed as described for Table I. Percentage weight values are given at 5% moisture. Mean comparisons that were not significant at the 10% level (probT, homoscedastic *t* test ≤ 0.1; Microsoft Excel) are indicated by ns. nd, Not detected.

Plant	Value	Fru	Glc	Suc	Galactinol + Raffinosaccharides	Total Soluble Sugars	Starch	Protein	Oil	Protein + Oil	Soluble Sugars + Starch	Seed Weight
												μg
K46564	Mean	0.05	1.25	1.70	0.75	3.8	0.027	25.3	30.3	55.6	3.8	23.6
	SD	0.01	0.04	0.02	0.09	0.0	0.004	0.6	1.4			0.3
Wild type	Mean	0.06	0.93	1.92	0.62	3.5	0.016	21.9	37.0	58.9	3.5	25.8
	SD	0.01	0.05	0.03	0.06	0.1	0.014	0.2	0.3			0.3
	Percentage change	−13 (ns)	35	−12	17	6	74	16	−18	−14	6	−9
K46562	Mean	0.06	1.03	2.01	0.71	3.8	nd	22.1	35.3	57.4	3.8	20.6
	SD	0.02	0.10	0.05	0.12	0.1		0.1	0.7			1.7
Wild type	Mean	0.06	0.92	1.89	0.62	3.5	0.006	20.9	38.9	59.8	3.5	22.9
	SD	0.00	0.02	0.03	0.06	0.1	0.010	0.5	1.6			1.3
	Percentage change	−8 (ns)	12 (ns)	6 (ns)	14 (ns)	9		5	−9	−14	8	−10 (ns)

mediated Glc-6-P synthesis effectively bypasses reduced flux through UGPase, thus supporting higher levels of starch biosynthesis in plastids of developing seed (Barratt et al., 2009). Increased levels of transient starch and free hexoses indicates that reduced flux through PFP due to PPi substrate depletion is most likely responsible for reduced oil accumulation in lines with increased expression of cytosolic PPiase enzymes. Alternative routes of oil precursor supply via cytosolic glycolysis initiated by ATP-dependent phosphofructokinase or plastidic mobilization of sugars, derived from the transient starch pool or hexose-phosphate import, cannot fully compensate for reduced flux through PPi-dependent cytosolic glycolysis. Unaltered or increased protein accumulation in mature seeds of transgenic lines with increased levels of cytosolic PPiase enzyme suggests the existence of pathways, active at later stages of seed maturation, that provide carbon skeletons for amino acid biosynthesis that are unaffected by reduced PPi substrate supply.

Our current model would suggest that seed oil accumulation is highly sensitive to cytosolic PPi levels, which could furthermore imply that increasing cytosolic PPi supply during seed maturation may provide a metabolic engineering strategy to increase seed storage lipid accumulation. To further test this model, we generated lines with tissue-specific RNAi of cytosolic PPiase genes. In addition to At1g01050, there are four additional PPiase genes in Arabidopsis that encode proteins that share at least 70% amino acid sequence identity and lack clearly identifiable signal peptides. Closely related, orthologous genes encoding proteins that show a similar level of sequence identity to At1g01050 are easily identified in higher plants, including crop plants with completely sequenced genomes belonging to monocot and dicot classes (Fig. 6).

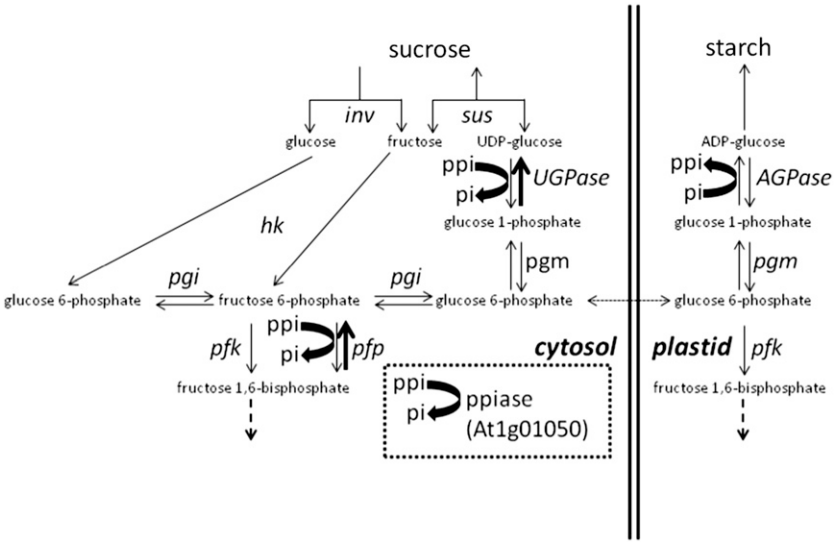

Figure 5. Simplified scheme of reactions of Suc mobilization, interconversions within the hexose-phosphate pool, starch biosynthesis, and early reactions of glycolysis during Arabidopsis seed maturation. AGPase, ADP-Glc pyrophosphorylase; pfk, ATP-dependent phosphofructokinase; pfp, pyrophosphate-dependent phosphofructokinase; pgi, phosphoglucoisomerase; pgm, phosphoglucomutase; ppi, pyrophosphate; ppiase, pyrophosphatase; sus, Suc synthase; inv, invertase.

Analysis of cytosolic PPiase gene expression in Arabidopsis at http://bar.utoronto.ca/ (Winter et al., 2007) indicates that two cytosolic PPiase genes, At1g01050 (PPA1) and At3g53620 (PPA4), show significant expression during the seed maturation phase.

Transgenic lines generated with a construct, pKR92-PPA hairpin (HP; Supplemental Fig. S3), directing RNAi of At1g01050 and At3g53620 during seed maturation show a heritable increase of seed oil content ranging from 1% to 4% (Fig. 7; Table V). We previously generated transgenic lines with a construct for seed-preferred RNAi, pKR1482-PPA1, which is only composed of coding sequences of At1g01050 (Supplemental Fig. S4). As At1g01050 and At3g53620 share 78% DNA sequence identity, including stretches of DNA sequence of greater than 21 nucleotides, it is likely that events generated with pKR1482-PPA1 will show silencing of both PPiase genes expressed during seed maturation. In keeping with this, the pKR1482-PPA1 construct also produced events with a heritable increase of seed oil

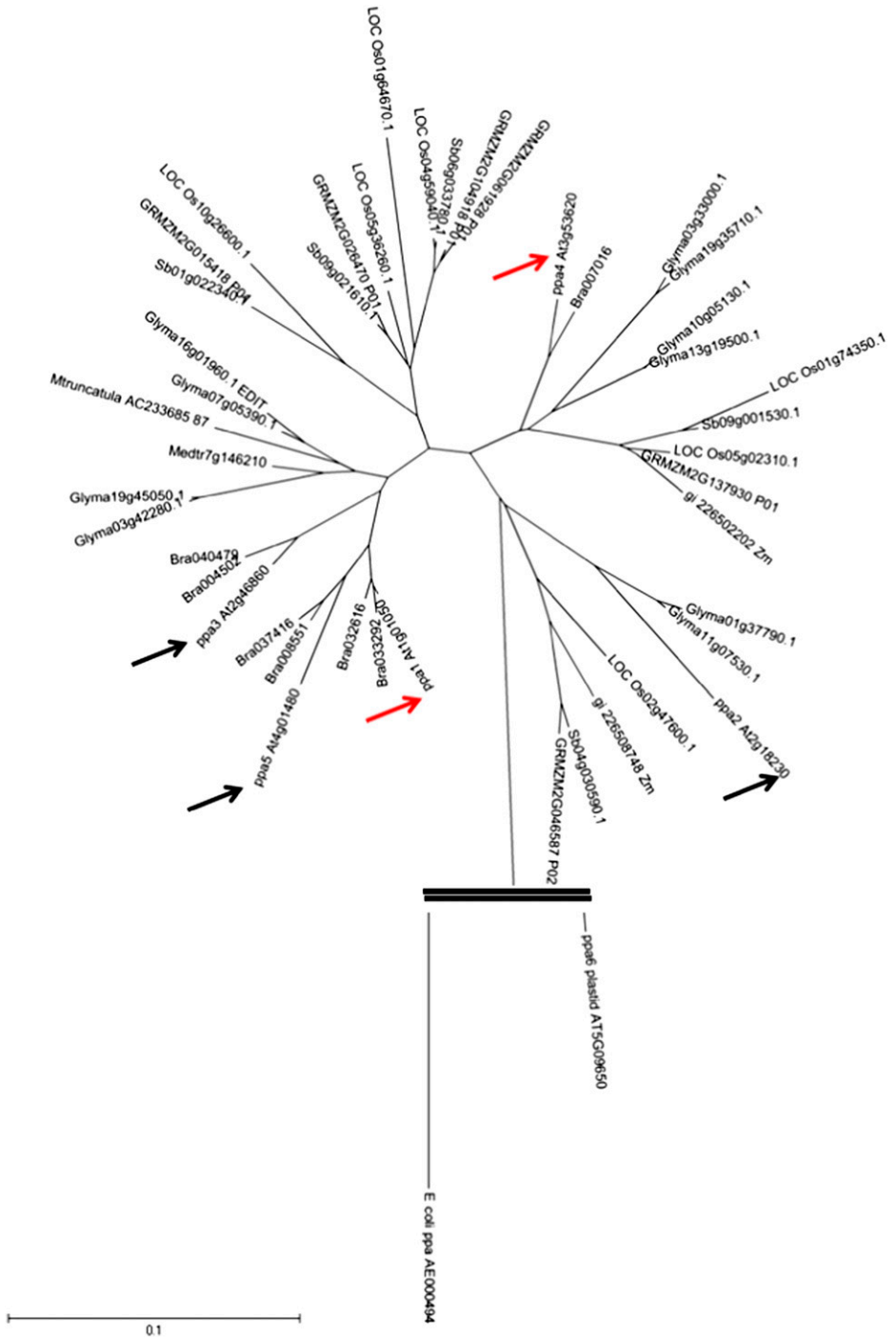

Figure 6. Phylogenetic tree based on a MUSCLE alignment (Edgar, 2004) of deduced amino acid sequences of cytosolic Arabidopsis PPiases and orthologs identified in completed genome sequences of *B. rapa*, soybean, *M. truncatula*, sorghum, rice, and maize. A plastidic PPiase gene of Arabidopsis and an *E. coli* PPiase gene were used as outgroups. Arrows indicate Arabidopsis sequences. Red arrows indicate Arabidopsis genes expressed during seed maturation based on expression analysis at http://bar.utoronto.ca/ (Winter et al., 2007). The evolutionary history was inferred using the neighbor-joining method (Saitou and Nei, 1987). The optimal tree with the sum of branch length = 2.98397151 is shown. The tree is drawn to scale, with branch lengths in the same units as those of the evolutionary distances used to infer the phylogenetic tree. The evolutionary distances were computed using the Poisson correction method (Zuckerkandl and Pauling, 1965) and are in units of the number of amino acid substitutions per site. The analysis involved 46 amino acid sequences. All positions containing gaps and missing data were eliminated. There were 160 positions in the final data set. Evolutionary analyses were conducted in MEGA5 (Tamura et al., 2011). [See online article for color version of this figure.]

Figure 7. Seed oil content of T1 plants generated with a construct for silencing of At1g01050 and At3g53620 under the control of the seed-preferred GY1 promoter (diamonds) and untransformed wild-type control plants (squares). Events with increased oil content that were advanced to T2 grow-out and seed oil analysis (Table V) are bracketed.

content of 1.5% to 3% (data not shown). Mature T3 seed of three events, K14700, K46696, and K46698, generated with this construct were subjected to analysis of seed composition (Table VI). In mature seed of these events, the oil increase is associated with a decrease in protein content whereas soluble carbohydrate levels are unchanged.

In summary, we have shown that modulation of cytosolic pyrophosphatase activity exerts significant control over glycolytic mobilization of Suc for seed oil biosynthesis. The increased seed oil phenotype of events with seed-preferred RNAi of genes encoding cytosolic PPiase enzymes suggests that the availability of cytosolic pyrophosphate alone limits the utilization of Suc for seed oil biosynthesis. We infer from this that cytosolic PPiase activity (and most likely PPi levels) during the seed maturation phase are not perfectly coordinated with PPi needs by forward reactions of the cytosolic UGPase and PFP enzymes. Down-regulation of PPiase gene expression most likely increases oil biosynthesis by means of improved flux through PPi-dependent reactions of cytosolic glycolysis that support oil biosynthesis. The function of cytosolic PPiase enzyme activity during the maturation phase of oil seed filling remains mostly enigmatic at this point but could include a role in maintaining cytosolic PPi homeostasis by acting in conjunction with PFP, UGPase, and H^+-translocating PPiases (Stitt, 1998; Heinonen, 2001). We have not observed any evidence of reduced seed yield or germination defects in events harboring constructs with seed-preferred RNAi of PPiase genes (K. Meyer, unpublished data), which may indicate that PPiase activity during seed maturation is not essential or that there is significant functional redundancy.

DISCUSSION

Role of Pyrophosphatases in Metabolism

PPi is generated in all prokaryotic and eukaryotic cells in many anabolic reactions, including the synthesis of macromolecules such as proteins, DNA, RNA, and starch (Heinonen, 2001). In many cases, the role of PPiase enzymes is to keep the equilibrium of these biosynthetic reactions on the side of the product by hydrolysis of the coproduct of the anabolic reaction. In keeping with this role, loss-of-function mutations of genes encoding PPiases are not viable in certain prokaryotes (Chen et al., 1990).

Role of Cytosolic Pyrophosphatases in Plant Metabolism

Subcellular fractionation of photosynthetic plant tissues indicates that PPi levels are very low in plastids due to high levels of PPiase activity detected in this organelle. In contrast, PPi levels are in the 0.1 to 0.3 mM range in the cytosol, which is commonly explained by the inability to detect PPiase activity in this cell fraction (Weiner et al., 1987; Stitt, 1998). The role of pyrophosphate in plant metabolism has been studied in detail mostly in the context of carbohydrate metabolism. Transient starch biosynthesis in the plastid generates PPi during the synthesis of ADP-Glc by ADP-Glc pyrophosphorylase. In cytosolic energy metabolism, PPi levels are modulated by the combined activity of UGPase, PFP, and membrane-bound, vacuolar H^+-translocating PPiases (Heinonen, 2001).

The role of cytosolic PPi in plant carbohydrate metabolism has been investigated using transgenic plants expressing an *E. coli* PPiase gene product in the cytosol (Jelitto et al., 1992; Sonnewald, 1992; Lee et al., 2005). Constitutive expression leads to pleiotropic growth defects and increased accumulation of Suc, hexoses, nucleotide sugars, and transient starch in photosynthetic tissues. In potato (*Solanum tuberosum*) tubers, a nonphotosynthetic sink tissue, constitutive expression of heterologous PPiase activity increases the levels of soluble sugars including Suc, but in contrast to photosynthetic tissues, increased levels of nucleotide sugars are accompanied by increased rates of Suc degradation and starch accumulation (Geigenberger et al., 1998). The increased levels of hexoses and nucleotide sugars in

Table V. *Comparative analysis of seed oil content of events generated with construct for seed-preferred RNAi of At1g01050 and At3g53620 and untransformed wild-type control plants*

Twenty-four T2 plants of each event were grown in 36-cell flats alongside 12 wild-type plants. Dry seed were harvested from individual plants. Seed oil content was measured by ^{1}H-NMR. All comparisons were significant at the 10% level (probT, homoscedastic *t* test $\leq$ 0.1; Microsoft Excel).

Event	Average Percentage Oil, Transgenic	Average Percentage Oil, Wild Type	Percentage Change
K61344	40.9	37	3.9
K61355	43	39.4	3.6
K61345	43.1	41.2	1.9
K61346	41.9	40.6	1.3
K61353	43.4	42.4	1

Table VI. *Composition of mature T3 seed of three events generated with pKR1482-PPA1 and untransformed wild-type control plants*

Plants of each event were grown in the same 36-cell flat alongside wild-type plants. Seeds were bulk harvested by type and homogenized and analyzed as described above. Percentage weight values are given at 5% moisture. Mean comparisons that were not significant at the 10% level (probT, homoscedastic *t* test ≤ 0.1; Microsoft Excel) are indicated by ns. nd, Not detected.

Plant	Value	Fru	Glc	Suc	Raffinosaccharides	Total Soluble Sugars	Starch	Protein	Oil (NMR)
K14700	Mean	0.04	0.31	1.56	0.18	2.1	nd	17.5	41.4
	SD	0.00	0.02	0.01	0.00	0.0		0.0	
Wild type	Mean	0.04	0.42	1.56	0.19	2.2	nd	19.3	38.9
	SD	0.00	0.08	0.02	0.01	0.1		0.1	
	Percentage change	−2 (ns)	−37	0	−4 (ns)	−6		−11	6
K46696	Mean	0.04	0.33	1.51	0.16	2.0	nd	16.0	44.4
	SD	0.00	0.02	0.01	0.00	0.0		0.2	
Wild type	Mean	0.04	0.35	1.62	0.18	2.2	nd	18.7	42.2
	SD	0.00	0.01	0.03	0.00	0.0		0.1	
	Percentage change	11	−5 (ns)	−7	−11	−7		−17	5
K46698	Mean	0.04	0.30	1.52	0.19	2.1	nd	15.4	45.4
	SD	0.00	0.02	0.02	0.01	0.0		0.2	
Wild type	Mean	0.04	0.41	1.57	0.20	2.2	nd	17.7	43.3
	SD	0.00	0.08	0.03	0.00	0.1		0.2	
	Percentage change	5 (ns)	−38	−3 (ns)	−4	−8		−15	5

source tissues and reduced sink strength in nonphotosynthetic tissues (Jelitto et al., 1992) are consistent with a role of PPi as an energy donor to the forward reactions of UGPase and PFP in cytosolic Suc catabolism. Changes of carbohydrate profiles in response to cytosolic expression of heterologous PPiase enzymes differ between plant tissues and plant species and may reflect different abilities of a given plant tissue to bypass the blockage of sucrose synthase (SUS)-mediated Suc catabolism using ATP-dependent pathways initiated by invertase-mediated sucrolysis.

Disruption of a vacuolar H^+-translocating PPiase (At1g15690) leads to a postgermination growth defect that can be rescued by supplementation of Suc or cytosolic expression of a soluble yeast pyrophosphatase. This supports the essential role of cytosolic PPiase activity controlling the equilibrium of gluconeogenic reactions in the heterotrophic growth phase of early seedling establishment (Ferjani et al., 2011).

Role of Pyrophosphatases in Seed Filling

There are many examples providing only indirect evidence for the role of PPi as an energy source driving cytosolic reactions of Suc mobilization to provide precursors for oil biosynthesis in developing seeds. This includes the demonstration of hypoxic, ATP-limited conditions during seed fill (Vigeolas et al., 2003; Musgrave et al., 2008; Borisjuk and Rolletschek, 2009), the high expression of SUS, UGPase, and PFP genes and enzymes during the maturation phase of seed filling (Baud and Graham, 2006; Troncoso-Ponce et al., 2011), and the fact that SUS and PFP genes respond to WRI1 expression (Focks and Benning, 1998; Ruuska et al., 2002). Thus, the use of PPi appears to be part of an ATP-saving, SUS-initiated pathway of cytosolic Suc catabolism characteristic of the maturation phase of seed development with highest rates of seed storage compound accumulation. However, direct, genetic evidence for the essential nature of the pathway in Arabidopsis seed filling is lacking, as SUS quadruple mutants show wild-type levels of oil and protein in dry seed and only a transient obstruction of seed fill is observed in developing seed of SUS mutants (Barratt et al., 2009; Angeles-Núñez and Tiessen, 2010). Moreover, to our knowledge, no other mutants with altered seed composition have been described that carry loss-of-function alleles of genes encoding components of this pathway.

We acknowledge that the compositional phenotype of immature siliques or seed of the lo15571 mutant and GY1::At1g01050 events is somewhat reminiscent of the tuber phenotype of potato plants expressing heterologous PPiase enzymes in the cytosol (Geigenberger et al., 1998). However, it should be noted that we are altering the expression of an endogenous cytosolic pyrophosphate enzyme (instead of introducing a heterologous enzyme that may operate in an unregulated mode). Thus, we provide, to our knowledge for the first time, direct evidence for the role of transcriptional control of endogenous cytosolic plant pyrophosphatase enzymes in the metabolic regulation of seed filling. Even though plant genome sequencing and transcriptional profiling of plant tissues, including developing seeds, predict the existence of closely related gene families encoding cytosolic pyrophosphatase enzymes, direct evidence for the regulatory role of these enzymes has been generally lacking to this point. Our results suggest that cytosolic PPiase activity is a crucial determinant of the rate of cytosolic glycolysis. Increased expression of the PPiase enzyme

during seed fill only leads to a small increase in Suc but a more significant increase in hexoses and/or transient starch. This emphasizes the role of PPi in controlling rates of glycolysis via PFP-mediated reactions while the use of PPi by UGPase is effectively bypassed, thus leading to unaltered rates of Suc mobilization (i.e. sink strength in developing seed). A role of PFP in the control of PPi homeostasis has been proposed due to its dual role in PPi consumption and synthesis (Taiz, 1986; Dancer and ap Rees, 1989; Stitt, 1998; Heinonen, 2001). In the latter reaction, ATP is converted to PPi when Fru-1,6-bisP synthesized by phosphofructokinase is converted to Fru-6-P (Fig. 5). Increased futile cycling through these reactions may be promoted by increased cytosolic PPiase activity in the cytosol, thus restricting the cytosolic catabolism of sugars.

Our findings also further clarify the relative contribution of cytosolic and plastidic glycolysis in the provision of precursors for oil biosynthesis in developing seed, emphasizing the importance of the former. This complements results from metabolic flux analysis, which is not always able to resolve this aspect of seed filling due to the rapid exchange of labeled glycolytic intermediates between plastidic and cytosolic compartments (Schwender et al., 2003).

CONCLUSION

We report here the important role of cytosolic pyrophosphatase enzyme expression in cytosolic glycolysis, specifically its role providing carbon for seed storage lipid accumulation. Clearly, we are only at the beginning of understanding the biochemical basis of the compositional shift observed in response to changes in cytosolic PPiase expression. Future work needs to examine how levels of PPi, hexose phosphates, and nucleotide sugars are related to altered seed storage compound accumulation. There is an opportunity for MFA to investigate how the route providing precursors for seed storage protein is modified in response to altered PPiase expression. Overall, this study provides a novel, promising target for the modification of seed storage accumulation for applications in plant biotechnology.

MATERIALS AND METHODS

Plant Growth Conditions

Arabidopsis (*Arabidopsis thaliana*) plants were grown in controlled environments, 22°C, 150 to 200 μE m^{-1} s^{-1}, under permanent illumination for 6 to 7 weeks. Prior to seed harvest, plant dry-down was performed for 1 to 2 weeks at 25°C at elevated light intensity (250–300 μE m^{-1} s^{-1}).

Density Gradient Screening

A method for screening Arabidopsis seed density was modified from Focks and Benning (1998). Density layers were prepared by a mixture of 1,6-dibromohexane (d = 1.6), 1-bromohexane (d = 1.17), and mineral oil (d = 0.84) at different ratios. From the bottom to the top of the tube, six layers of organic solvents each composed of 2 mL were added sequentially. The ratios of 1,6-dibromohexane:1-bromohexane:mineral oil for each layer were 1:1:0, 1:2:0, 0:1:0, 0:5:1, 0:3:1, and 0:0:1. About 600 mg of T3 seed of a given pool of 96 activation-tagged lines, corresponding to about 30,000 seeds, was loaded onto the surface layer of a 15-mL glass tube containing said step gradient. After centrifugation for 5 min at 2,000*g*, seeds were separated according to their density. The seeds in the lower two layers of the step gradient and from the bottom of the tube were collected. Organic solvents were removed by sequential washing with 100% and 80% ethanol, and seeds were sterilized using a solution of 5% hypochloride in water. Seed were rinsed in sterile water and plated on Murashige and Skoog medium composed of 0.5× Murashige and Skoog salts, 1% Suc, 0.05% (w/v) MES/KOH (pH 5.8), 10 g L^{-1} agar, and 15 mg L^{-1} glufosinate ammonium (Sigma-Aldrich). A total of 520 T3 pools each derived from 96 T2 activation-tagged lines were screened in this manner. Seed pool 225, when subjected to density gradient centrifugation as described above, produced about 20 seed with increased density. These seed were sterilized and plated on selective medium. Seedlings were transferred to soil 2 weeks after plating and grown in the same 36-cell flat alongside wild-type control plants.

NMR-Based Analysis of Seed Oil Content

Seed oil content was determined using a Maran Ultra NMR analyzer (Resonance Instruments). Samples (e.g. batches of Arabidopsis seed ranging in weight between 5 and 200 mg) were placed into preweighed 2-mL polypropylene tubes (Corning) previously labeled with unique bar code identifiers. Samples were then placed into 96-place carriers and processed by an ADEPT COBRA 600 SCARA robotic system. Oil content (on a percentage weight basis) of Arabidopsis tissue was calculated as follows: mg oil = (NMR signal − 2.1112)/37.514; % oil = ([mg oil]/1,000)/(g of seed sample weight) × 100. Prior to establishing this formula, Arabidopsis seed oil was extracted as follows. Approximately 5 g of mature Arabidopsis seed (cv Columbia) was ground to a fine powder using a mortar and pestle. The powder was placed into a 33- × 94-mm paper thimble (Ahlstrom), and the oil was extracted during approximately 40 extraction cycles with petroleum ether (boiling point 39.9°C–51.7°C) in a Soxhlet apparatus. The extract was allowed to cool, and the crude oil was recovered by removing the solvent under vacuum in a rotary evaporator. Calibration parameters were determined by precisely weighing 11 standard samples of partially purified Arabidopsis oil (samples contained 3.6, 6.3, 7.9, 9.6,12.8, 16.3, 20.3, 28.2, 32.1, 39.9, and 60 mg of partially purified Arabidopsis oil) into 2-mL polypropylene tubes (Corning) and subjecting them to NMR analysis. A calibration curve of oil content (percentage seed weight basis) to NMR value was established.

Compositional Analysis

Tissue Preparation

Arabidopsis seed (approximately 0.5 g in a 0.5- × 2-inch polycarbonate vial) was ground to a homogeneous paste in a GENOGRINDER (three times for 30 s each at 1,400 strokes per minute, with a 15-s interval between each round of agitation). After the second round of agitation, the vials were removed and the Arabidopsis paste was scraped from the walls with a spatula prior to the last burst of agitation. Developing siliques were harvested into liquid N_2 and stored at −80°C prior to analysis. Frozen developing silique tissue was ground to a fine powder and lyophilized.

Determination of Protein Content

Protein contents were estimated by combustion analysis on a Thermo Finnigan Flash 1112EA combustion analyzer running in the nitrogen-carbon-sulfur mode (vanadium pentoxide was omitted) according to the instructions of the manufacturer. Triplicate tissue samples of 4 to 8 mg were used for analysis. Protein contents were calculated by multiplying percentage nitrogen, determined by the analyzer, by 6.25. Protein contents were expressed on a percentage tissue weight basis.

Determination of Oil Content

Triplicate tissue samples, 20 to 50 mg, were weighed into 13- × 100-mm glass tubes. Gravimetric analysis of oil content was performed by adding 2-mL aliquots of heptane to each tube. The tubes were vortex mixed and placed into an

ultrasonic bath filled with water heated to 60°C. The samples were sonicated at full power (approximately 360 W) for 15 min and then centrifuged (5 min, 1,700*g*). The supernatants were transferred to clean tubes and the pellets were extracted two more times with heptane (2 mL, second extraction; 1 mL, third extraction), with the supernatants from each extraction being pooled. After lipid extraction, 1 mL of acetone was added to the pellets, and after vortex mixing, to fully disperse the material, they were taken to dryness in a SpeedVac.

Soluble Carbohydrate Extraction

Two milliliters of 80% ethanol was added to the dried pellets from above. The samples were thoroughly vortex mixed until the plant material was fully dispersed in the solvent prior to sonication at 60°C for 15 min. After centrifugation for 5 min at 1,700*g*, the supernatants were decanted into clean 13- × 100-mm glass tubes. Two more extractions with 80% ethanol were performed, and the supernatants from each were pooled. The extracted pellets were suspended in acetone and dried (as above). A total of 100 μL of 5 mg mL^{-1} β-phenyl glucopyranoside was added to each extract prior to drying in a SpeedVac.

Starch Extraction

The acetone-dried powders from above were suspended in 0.9 mL of MOPS buffer (50 mM MOPS and 5 mM $CaCl_2$, pH 7.0) containing 100 units of heat-stable α-amylase (from *Bacillus licheniformis*; Sigma). Samples were placed in a heat block (90°C) for 75 min and vortex mixed every 15 min. Samples were then allowed to cool to room temperature, and 0.6 mL of acetate buffer (285 mM, pH 4.5) containing 5 units of amyloglucosidase (Roche) was added to each. Samples were incubated for 15 to 18 h at 55°C in a water bath fitted with a reciprocating shaker; standards of soluble potato (*Solanum tuberosum*) starch (Sigma) were included to ensure that starch digestion went to completion. Postdigestion, the released carbohydrates were extracted as described above.

Sample Derivatization and Analysis

The dried samples from the soluble sugar and starch extractions described above were solubilized in anhydrous pyridine (Sigma-Aldrich) containing 30 mg mL^{-1} hydroxylamine-HCl (Sigma-Aldrich). Samples were placed on an orbital shaker (300 rpm) overnight and then heated for 1 h (75°C) with vigorous vortex mixing applied every 15 min. After cooling to room temperature, 1 mL of hexamethyldisilazane (Sigma-Aldrich) and 100 μL of trifluoroacetic acid (Sigma-Aldrich) were added. The samples were vortex mixed, and the precipitates were allowed to settle prior to transferring the supernatants to gas chromatography sample vials. Samples were analyzed on an Agilent 6890 gas chromatograph fitted with a DB-17MS capillary column (15-m × 0.32-mm × 0.25-μm film). Inlet and detector temperatures were both 275°C. After injection (2 μL, 20:1 split), the initial column temperature (150°C) was increased to 180°C at a rate of 3°C min^{-1} and then at 25°C min^{-1} to a final temperature of 320°C. The final temperature was maintained for 10 min. The carrier gas was hydrogen at a linear velocity of 51 cm s^{-1}. Detection was by flame ionization. Data analysis was performed using Agilent ChemStation software. Each sugar was quantified relative to the internal standard, and detector responses were applied for each individual carbohydrate (calculated from standards run with each set of samples). Final carbohydrate concentrations were expressed on a tissue weight basis. Carbohydrates were identified by retention time matching, with authentic samples of each sugar run in the same chromatographic set, and by gas chromatography-mass spectrometry, with spectral matching to the National Institute of Standards and Technology Mass Spectral Library version 2a, build July 1, 2002.

Determination of DNA Sequence Flanking the T-DNA Insertion

An adaptor was generated by annealing primers AD1 (5′-GCTATCGGTAATGCGTCACAAGCGTGAACAATGAGTAATGATA-3′) and AD2 (5′-CGCACTTGTTACTCATTACTAT-3′). Genomic DNA was isolated from lyophilized seedling tissue of lo15571. Genomic DNA of lo15571 flanking the left border of pHSbarENDs2 (Supplemental Fig. S1) was amplified by SAIFF exactly as described by Muszynski et al. (2006) using genomic DNA digested with *Alu*I, the adaptor described above, and primers A (5′-CCATTTGGACGTGAATGTAGACACGTCGA-3′) and B (5′-GCTATCGGTAATGCGTCA-3′) in the first PCR and primers C (5′-TGCTTTCGCCTATAAATACGACGGATCGT-3′) and D (5′-GCGTCACAAGCGTGAACA-3′) in the second PCR. PCR products were cloned and sequenced.

Plant Transformation Vectors

Construction of a Binary Vector for Seed-Preferred Expression of At1g01050

Primers At1g01050 FWD (5′-CACCATGGCCACCGCTTCAATCTTCCCCGC-3′) and At1g01050 REV (5′-GCGGCCGCTTATTCGCTCCAGTACTTCTC-3′) were used to amplify the At1g01050 ORF from a cDNA library of developing Arabidopsis seeds. The PCR product was cloned into pENTR (Invitrogen) to give pENTR-PPA1. The PPA1 ORF was inserted in the sense orientation downstream of the GY1 promoter in the binary plant transformation vector pKR1478 (Meyer and Everard, 2011) using Gateway LR recombinase (Invitrogen) using the manufacturer's instructions to give pKR1478-PPA1 (Supplemental Fig. S2).

Construction of a Plasmid for Seed-Preferred RNAi of At1g01050 and At3g53620

Primer pairs SA325 (5′-GCGGCCGCCATGATCTCGAGATAGGACCTG-3′)/SA326 (5′-TCTAGACAAAGAAACGGCGGATCTCAGCCA-3′) and SA329 (5′-GAATTCGCGGCCGCCATGATCTCGAGATAGGACCTGAA-3′)/SA330 (5′-CTGCAGCAAAGAAACGGCGGATCTCAGCCA-3′) were used to amplify a fragment of the At3g53620 ORF from a cDNA library of developing Arabidopsis seeds that is flanked by *Not*I, *Xba*I, *Pst*I, and *Eco*RI restriction sites, respectively. The PCR products were cloned into pBSKS+ (Stratagene) to give pBSKS-PPA4-TR1A and pBSKS-PPA4-TR1B, respectively. Primers SA327 (5′-TCTAGACGACCAGCTCCTCGTCTTAACGAG-3′) and SA328 (5′-GGATCCTCAGGGTGTGGAGAATGTATTCAG-3′) were used to amplify a fragment of the At1g01050 ORF from a cDNA library of developing Arabidopsis seeds that is flanked by *Xba*I and *Bam*HI. The PCR product was cloned into pBSKS+ (Stratagene) to give pBSKS-PPA1-TR1+TR2. Primers SA331 (5′-CTGCAGCGACCAGCTCCTCGTCTTAACGAG-3′) and SA332 (5′-GGATCCAGAAAACAACCCGGAAGCACAGGT-3′) were used to amplify a fragment of the At1g01050 ORF from a cDNA library of developing Arabidopsis seeds that is flanked by *Pst*I and *Bam*HI. The PCR product was cloned into pBSKS+ (Invitrogen) to give pBSKS-PPA1-TR1. pBSKS-PPA4-TR1A was linearized with *Xba*I and *Bam*HI and ligated to a 0.6-kb fragment excised from pBSKS-PPA1-TR1+TR2 with *Xba*I and *Bam*HI to give pBSKS-PPA HP-A. pBSKS-PPA4-TR1B linearized with *Bam*HI and *Pst*I was ligated to a 0.3-kb fragment excised from pBSKS-PPA1-TR1 with the same restriction enzymes to give pBSKS-PPA HP-B. pBSKS-PPA HP-A linearized with *Bam*HI and *Eco*RI was ligated to a 0.75-kb fragment excised from pBSKS-PPA HP-B with the same enzymes to give pBSKS-PPA HP. The PPA HP cassette was inserted downstream of the GY1 promoter and upstream of the 3′ untranslated region of the soybean (*Glycine max*) Kunitz trypsin inhibitor gene (Jofuku and Goldberg, 1989). The RNAi expression cassette was excised with *Asc*I and ligated to *Asc*I-digested binary plant transformation vector pKR92 (Meyer et al., 2010) to give pKR92-PPA HP (Supplemental Fig. S3).

Construction of a Plasmid for Seed-Preferred RNAi of At1g01050

We used pENTR-PPA1 and the binary plant transformation vector pKR1482 (Meyer and Everard, 2011) to insert the PPA1 ORF in the sense and antisense orientations downstream of the GY1 promoter using Gateway LR recombinase (Invitrogen) using the manufacturer's instructions to give pKR1482-PPA1 (Supplemental Fig. S4).

All binary vectors were transformed into *Agrobacterium tumefaciens* strain NTL4 (Luo et al., 2001) by electroporation and used to transform Arabidopsis plants using the floral dip method (Zhang et al., 2006).

Immunological Methods

Expression Cloning of At1g01050

The At1g01050 ORF was amplified with primers PPA1 FWD (5′-CATATGAGTGAAGAAACTAAAGATAACC-3′) and PPA1 REV (5′-CTCGAGACGCCTCAGGGTGTGGAGAATG-3′) using plasmid DNA of pKR1478-PPA1. PCR products were cloned into pGEM T-Easy (Promega). The ORF was excised by digestion with *Nde*I and *Xho*I and ligated to *Nde*I- and *Xho*I-linearized pET29a to give pET29a-PPA1. Competent *Escherichia coli* cells of strain Rosetta(DE3)pLysS (Novagen/EMD Biosciences) were transformed with pET29a-PPA1 using electroporation. Eight 500-mL flasks each containing 250 mL of Luria-Bertani medium supplemented with 50 μg mL^{-1} kanamycin were

inoculated with strain Rosetta(DE3)pLysS carrying pET29a-PPA1. The cultures were grown at 37°C until a cell density (optical density λ = 600 nm) of 0.6 was achieved. The cultures were cooled to 22°C on ice. Isopropyl β-D-1-thiogalactopyranoside was then added to a final concentration of 0.2 mM followed by continued culture at 16°C for 36 h. Cells were harvested by centrifugation (5,000*g*, 10 min) and resuspended in 30 mL of 100 mM Tris-HCl (pH 7.5), 0.5 M NaCl, 0.5 mM EDTA, and 2 mM dithiothreitol. The cell suspension was passed twice through a French press and cleared by centrifugation (30,000*g*, 20 min, 4°C). The enzyme extract (30 mL) was buffer exchanged in 2.5-mL aliquots on PD10 columns (GE Healthcare) into 100 mM Tris-HCl, pH 7.5, and 500 mM NaCl. Buffer-exchanged extract (40 mL) was loaded onto a HiTrap chelating HP column with a 5-mL gel bed volume (GE Healthcare). The HiTrap chelating HP column had previously been charged with Ni^{2+} according to the manufacturer's instructions. The column was developed at a flow rate of 2 mL min^{-1} at 22°C as follows for solvent A (100 mM Tris-HCl [pH 7.5], 500 mM NaCl, and 20 mM imidazole) and solvent B (100 mM Tris-HCl [pH 7.5], 500 mM NaCl, and 500 mM imidazole): 0 to 20 min, 0% B; 20 to 35 min, 20% B; 35 to 50 min (linear gradient), 20% to 100% B; 50 to 55 min, 100% B; 55 to 60 min, 0% B. Fractions of 1.5 mL were collected from beginning to end of the linear imidazole gradient. Fractions of 10 μL were analyzed by SDS-PAGE. Fractions containing a protein of 25 kD were pooled and buffer exchanged into 20 mM Tris-HCl (pH 7.5) and 5% glycerol. Analysis of an overloaded PAGE gel indicates that the Ni^{2+} affinity-purified At1g01050 protein is more than 95% pure. In this manner, 80 mg of At1g01050 protein could be purified from 2 L of *E. coli* culture. Purified At1g01050 protein was used to raise antibodies in rabbits (Rockland Immunochemicals).

Immunoblot Detection of Atg01050

Developing siliques, bulk harvested 4 weeks after transfer to soil, were homogenized in 100 mM Tris-HCl (pH 7.5), 0.5 M NaCl, 0.5 mM EDTA, and 2 mM dithiothreitol. The homogenate was cleared by centrifugation (30,000*g*, 20 min, 4°C), and the cell-free extract was buffer exchanged into 20 mM Tris-HCl (pH 7.5) and 5% glycerol. Proteins were separated by PAGE using 10% NuPAGE Bis-Tris gels (Invitrogen) transferred to nitrocellulose membranes using the iBlot electroblotting system (Invitrogen). Western blots were developed using 1:1,000 and 1:5,000 dilutions of primary and secondary antibodies, respectively, and the BM chemiluminescence detection kit (Roche Diagnostics).

Phylogenetic Analysis

Predicted amino acid sequences of At1g01050 and the four closely related homologs At2g18230, At2g46860, At3g53620, and At4g01480 were used to search the following genome sequences: for maize (*Zea mays*), public maize B73 peptides from the 5b release of the public projects filtered gene set (www.maizesequence.org); for rice (*Oryza sativa*), predicted protein sequences from rice gene models (*japonica* group)-Michigan State University Rice Genome Annotation Project Osa1 release 7 (October 2011); for sorghum (*Sorghum bicolor*), predicted proteins from the sorghum Joint Genome Institute genomic sequence, version 1.4; for soybean, predicted proteins from predicted coding sequences from the soybean Joint Genome Institute Glyma1.01 genomic sequence; for *Medicago truncatula* and *Brassica rapa*, Phytozome 8.0 (http://www.phytozome.net/). Phytozome is a joint project of the Department of Energy's Joint Genome Institute and the Center for Integrative Genomics.

Supplemental Data

The following materials are available in the online version of this article.

Supplemental Figure S1. Simplified map of the enhancer tagging vector used to generate lo15571.

Supplemental Figure S2. Simplified map of binary vector for expression At1g01050 during seed maturation.

Supplemental Figure S3. Simplified map of binary vector for RNAi of At1g01050 and At3g53620 during seed maturation.

Supplemental Figure S4. Simplified map of binary vector for RNAi of At1g01050 during seed maturation.

ACKNOWLEDGMENTS

We thank Hajime Sakai and Amanuel Kiflemariam (Pioneer, A DuPont Company, Agricultural Biotechnology, Wilmington, DE) for access to enhancer tag libraries of Arabidopsis; Amitabh Mohanti and Rupa Raja (DuPont Knowledge Center, Hyderabad, India) for conducting SAIFF PCR analysis; and Alfred Ciuffetelli, Sheila Chadman, Kouame Adou, and Bruce Schweiger (Pioneer, A DuPont Company, Agricultural Biotechnology) for skillful technical assistance.

Received April 4, 2012; accepted May 4, 2012; published May 7, 2012.

LITERATURE CITED

Allen DK, Libourel IGL, Shachar-Hill Y (2009a) Metabolic flux analysis in plants: coping with complexity. Plant Cell Environ **32:** 1241–1257

Allen DK, Ohlrogge JB, Shachar-Hill Y (2009b) The role of light in soybean seed filling metabolism. Plant J **58:** 220–234

Alonso AP, Dale VL, Shachar-Hill Y (2010) Understanding fatty acid synthesis in developing maize embryos using metabolic flux analysis. Metab Eng **12:** 488–497

Andre C, Froehlich JE, Moll MR, Benning C (2007) A heteromeric plastidic pyruvate kinase complex involved in seed oil biosynthesis in *Arabidopsis*. Plant Cell **19:** 2006–2022

Angeles-Núñez JG, Tiessen A (2010) Arabidopsis sucrose synthase 2 and 3 modulate metabolic homeostasis and direct carbon towards starch synthesis in developing seeds. Planta **232:** 701–718

Barratt DHP, Derbyshire P, Findlay K, Pike M, Wellner N, Lunn J, Feil R, Simpson C, Maule AJ, Smith AM (2009) Normal growth of Arabidopsis requires cytosolic invertase but not sucrose synthase. Proc Natl Acad Sci USA **106:** 13124–13129

Baud S, Dubreucq B, Miquel M, Rochat C, Lepiniec L (2008) Storage reserve accumulation in Arabidopsis: metabolic and developmental control of seed filling. The Arabidopsis Book **6**: e0113, doi/10.1199/tab.0113

Baud S, Graham IA (2006) A spatiotemporal analysis of enzymatic activities associated with carbon metabolism in wild-type and mutant embryos of Arabidopsis using in situ histochemistry. Plant J **46:** 155–169

Baud S, Mendoza MS, To A, Harscoët E, Lepiniec L, Dubreucq B (2007a) WRINKLED1 specifies the regulatory action of LEAFY COTYLEDON2 towards fatty acid metabolism during seed maturation in Arabidopsis. Plant J **50:** 825–838

Baud S, Wuillème S, Dubreucq B, de Almeida A, Vuagnat C, Lepiniec L, Miquel M, Rochat C (2007b) Function of plastidial pyruvate kinases in seeds of Arabidopsis thaliana. Plant J **52:** 405–419

Borisjuk L, Rolletschek H (2009) The oxygen status of the developing seed. New Phytol **182:** 17–30

Bourgis F, Kilaru A, Cao X, Ngando-Ebongue G-F, Drira N, Ohlrogge JB, Arondel V (2011) Comparative transcriptome and metabolite analysis of oil palm and date palm mesocarp that differ dramatically in carbon partitioning. Proc Natl Acad Sci USA **108:** 12527–12532

Cernac A, Benning C (2004) WRINKLED1 encodes an AP2/EREB domain protein involved in the control of storage compound biosynthesis in Arabidopsis. Plant J **40:** 575–585

Chen J, Brevet A, Fromant M, Lévêque F, Schmitter JM, Blanquet S, Plateau P (1990) Pyrophosphatase is essential for growth of Escherichia coli. J Bacteriol **172:** 5686–5689

Chen M, Thelen JJ (2011) Plastid uridine salvage activity is required for photoassimilate allocation and partitioning in *Arabidopsis*. Plant Cell **23:** 2991–3006

Dancer JE, ap Rees T (1989) Relationship between pyrophosphate:fructose-6-phosphate 1-phosphotransferase, sucrose breakdown, and respiration. J Plant Physiol **135:** 197–206

Edgar RC (2004) MUSCLE: multiple sequence alignment with high accuracy and high throughput. Nucleic Acids Res **32:** 1792–1797

Ferjani A, Segami S, Horiguchi G, Muto Y, Maeshima M, Tsukaya H (2011) Keep an eye on PPi: the vacuolar-type H^+-pyrophosphatase regulates postgerminative development in *Arabidopsis*. Plant Cell **23:** 2895–2908

Focks N, Benning C (1998) *wrinkled1*: a novel, low-seed-oil mutant of Arabidopsis with a deficiency in the seed-specific regulation of carbohydrate metabolism. Plant Physiol **118:** 91–101

Geigenberger P, Hajirezaei M, Geiger M, Deiting U, Sonnewald U, Stitt M (1998) Overexpression of pyrophosphatase leads to increased sucrose degradation and starch synthesis, increased activities of enzymes for sucrose-starch interconversions, and increased levels of nucleotides in growing potato tubers. Planta **205:** 428–437

Heinonen JK (2001) Biological Role of Inorganic Pyrophosphate. Kluwer Academic Publishers, Boston

Iida A, Nagasawa A, Oeda K (1995) Positive and negative cis-regulatory regions in the soybean glycinin promoter identified by quantitative transient gene expression. Plant Cell Rep **14:** 539–544

Jako C, Kumar A, Wei Y, Zou J, Barton DL, Giblin EM, Covello PS, Taylor DC (2001) Seed-specific over-expression of an Arabidopsis cDNA encoding a diacylglycerol acyltransferase enhances seed oil content and seed weight. Plant Physiol **126:** 861–874

Jelitto T, Sonnewald U, Willmitzer L, Hajirezeai M, Stitt M (1992) Inorganic pyrophosphate content and metabolites in potato and tobacco plants expressing E. coli pyrophosphatase in their cytosol. Planta **188:** 238–244

Jofuku KD, Goldberg RB (1989) Kunitz trypsin inhibitor genes are differentially expressed during the soybean life cycle and in transformed tobacco plants. Plant Cell **1:** 1079–1093

Koroleva OA, Tomlinson ML, Leader D, Shaw P, Doonan JH (2005) High-throughput protein localization in Arabidopsis using Agrobacterium-mediated transient expression of GFP-ORF fusions. Plant J **41:** 162–174

Lee J-W, Lee D-S, Bhoo SH, Jeon J-S, Lee Y-H, Hahn T-R (2005) Transgenic Arabidopsis plants expressing Escherichia coli pyrophosphatase display both altered carbon partitioning in their source leaves and reduced photosynthetic activity. Plant Cell Rep **24:** 374–382

Luo ZQ, Clemente TE, Farrand SK (2001) Construction of a derivative of Agrobacterium tumefaciens C58 that does not mutate to tetracycline resistance. Mol Plant Microbe Interact **14:** 98–103

Meyer K, Damude HG, Everard JD, Ripp KG, Stecca KL (2010) Use of a seed-specific sucrose synthase 2 promoter to drive ODP1 gene expression in cruciferous oilseed plants to increase oil content while maintaining normal germination. Patent Cooperation Treaty International Application No. WO 2010114989:A1

Meyer K, Everard JD (2011) Plant genes for cytosolic pyrophosphatases and their use in modifying seed storage compound content. Patent Cooperation Treaty International Application No. WO 2011008510:A2

Meyer K, Kinney AJ (2010) Biosynthesis and biotechnology of seed lipids including sterols, carotenoids and tocochromanols. *In* H Wada, N Murata, eds, Lipids in Photosynthesis, Vol 30. Springer, New York, pp 407–444

Musgrave M, Allen J, Blasiak J, Tuominen L, Kuang A (2008) In vitro seed maturation in Brassica rapa L.: relationship of silique atmosphere to storage reserve deposition. Environ Exp Bot **62:** 247–253

Muszynski MG, Dam T, Li B, Shirbroun DM, Hou Z, Bruggemann E, Archibald R, Ananiev EV, Danilevskaya ON (2006) *delayed flowering1* encodes a basic leucine zipper protein that mediates floral inductive signals at the shoot apex in maize. Plant Physiol **142:** 1523–1536

Navarro-De la Sancha E, Coello-Coutino MP, Valencia-Turcotte LG, Hernandez-Dominguez EE, Trejo-Yepes G, Rodriguez-Sotres R (2007) Characterization of two soluble inorganic pyrophosphatases from Arabidopsis thaliana. Plant Sci **172:** 796–807

Nielsen NC, Dickinson CD, Cho TJ, Thanh VH, Scallon BJ, Fischer RL, Sims TL, Drews GN, Goldberg RB (1989) Characterization of the glycinin gene family in soybean. Plant Cell **1:** 313–328

Periappuram C, Steinhauer L, Barton DL, Taylor DC, Chatson B, Zou J (2000) The plastidic phosphoglucomutase from Arabidopsis: a reversible enzyme reaction with an important role in metabolic control. Plant Physiol **122:** 1193–1199

Plaxton WC (1996) The organization and regulation of plant glycolysis. Annu Rev Plant Physiol Plant Mol Biol **47:** 185–214

Plaxton WC, Podesta FE (2006) The functional organization and control of plant respiration. Crit Rev Plant Sci **25:** 159–198

Pouvreau B, Baud S, Vernoud V, Morin V, Py C, Gendrot G, Pichon J-P, Rouster J, Paul W, Rogowsky PM (2011) Duplicate maize Wrinkled1 transcription factors activate target genes involved in seed oil biosynthesis. Plant Physiol **156:** 674–686

Roesler K, Shintani D, Savage L, Boddupalli S, Ohlrogge J (1997) Targeting of the Arabidopsis homomeric acetyl-coenzyme A carboxylase to plastids of rapeseeds. Plant Physiol **113:** 75–81

Ruan YL, Chourey PS (2006) Carbon partitioning in developing seed. *In* AS Basra, ed, Handbook of Seed Science and Technology. Haworth Press, Binghamton, NY, pp 125–152

Ruuska SA, Girke T, Benning C, Ohlrogge JB (2002) Contrapuntal networks of gene expression during *Arabidopsis* seed filling. Plant Cell **14:** 1191–1206

Ruuska SA, Schwender J, Ohlrogge JB (2004) The capacity of green oilseeds to utilize photosynthesis to drive biosynthetic processes. Plant Physiol **136:** 2700–2709

Saitou N, Nei M (1987) The neighbor-joining method: a new method for reconstructing phylogenetic trees. Mol Biol Evol **4:** 406–425

Santos-Mendoza M, Dubreucq B, Baud S, Parcy F, Caboche M, Lepiniec L (2008) Deciphering gene regulatory networks that control seed development and maturation in Arabidopsis. Plant J **54:** 608–620

Schauer SE, Jacobsen SE, Meinke DW, Ray A (2002) DICER-LIKE1: blind men and elephants in Arabidopsis development. Trends Plant Sci **7:** 487–491

Schwender J (2008) Metabolic flux analysis as a tool in metabolic engineering of plants. Curr Opin Biotechnol **19:** 131–137

Schwender J (2011) Experimental flux measurements on a network scale. Front Plant Physiol **2:** 63

Schwender J, Goffman F, Ohlrogge JB, Shachar-Hill Y (2004) Rubisco without the Calvin cycle improves the carbon efficiency of developing green seeds. Nature **432:** 779–782

Schwender J, Ohlrogge JB, Shachar-Hill A (2003) A flux model of glycolysis and the oxidative pentosephosphate pathway in developing Brassica napus embryos. J Biol Chem **278:** 29442–29453

Shen B, Allen WB, Zheng P, Li C, Glassman K, Ranch J, Nubel D, Tarczynski MC (2010) Expression of ZmLEC1 and ZmWRI1 increases seed oil production in maize. Plant Physiol **153:** 980–987

Shen B, Sinkevicius KW, Selinger DA, Tarczynski MC (2006) The homeobox gene GLABRA2 affects seed oil content in Arabidopsis. Plant Mol Biol **60:** 377–387

Shi L, Katavic V, Yu Y, Kunst L, Haughn G (2012) Arabidopsis glabra2 mutant seeds deficient in mucilage biosynthesis produce more oil. Plant J **69:** 37–46

Sonnewald U (1992) Expression of E. coli inorganic pyrophosphatase in transgenic plants alters photoassimilate partitioning. Plant J **2:** 571–581

Stitt M (1998) Pyrophosphate as an energy donor in the cytosol of plant cells: an enigmatic alternative to ATP. Bot Acta **111:** 167–175

Taiz L (1986) Are biosynthetic reactions in plant cells thermodynamically coupled to glycolysis and the tonoplast proton motive force? J Theor Biol **123:** 231–238

Tamura K, Peterson D, Peterson N, Stecher G, Nei M, Kumar S (2011) MEGA5: molecular evolutionary genetics analysis using maximum likelihood, evolutionary distance, and maximum parsimony methods. Mol Biol Evol **28:** 2731–2739

Tan H, Yang X, Zhang F, Zheng X, Qu C, Mu J, Fu F, Li J, Guan R, Zhang H, et al (2011) Enhanced seed oil production in canola by conditional expression of Brassica napus LEAFY COTYLEDON1 and LEC1-LIKE in developing seeds. Plant Physiol **156:** 1577–1588

Troncoso-Ponce MA, Kilaru A, Cao X, Durrett TP, Fan J, Jensen JK, Thrower NA, Pauly M, Wilkerson C, Ohlrogge JB (2011) Comparative deep transcriptional profiling of four developing oilseeds. Plant J **68:** 1014–1027

Vigeolas H, Hühn D, Geigenberger P (2011) Nonsymbiotic hemoglobin-2 leads to an elevated energy state and to a combined increase in polyunsaturated fatty acids and total oil content when overexpressed in developing seeds of transgenic Arabidopsis plants. Plant Physiol **155:** 1435–1444

Vigeolas H, van Dongen JT, Waldeck P, Huhn D, Geigenberger P (2003) Lipid storage metabolism is limited by the prevailing low oxygen concentrations within developing seeds of oilseed rape. Plant Physiol **133:** 2048–2060

Vigeolas H, Waldeck P, Zank T, Geigenberger P (2007) Increasing seed oil content in oil-seed rape (Brassica napus L.) by over-expression of a yeast glycerol-3-phosphate dehydrogenase under the control of a seed-specific promoter. Plant Biotechnol J **5:** 431–441

Weiner H, Stitt M, Heldt HW (1987) Subcellular compartmentation of pyrophosphate and alkaline pyrophosphatase in leaves. Biochim Biophys Acta **893:** 13–21

Winter D, Vinegar B, Nahal H, Ammar R, Wilson GV, Provart NJ (2007) An "electronic fluorescent pictograph" browser for exploring and analyzing large-scale biological data sets. PLoS ONE **2:** e718

Zhang X, Henriques R, Lin S-S, Niu Q-W, Chua N-H (2006) Agrobacterium-mediated transformation of Arabidopsis thaliana using the floral dip method. Nat Protoc **1:** 641–646

Zheng P, Allen WB, Roesler K, Williams ME, Zhang S, Li J, Glassman K, Ranch J, Nubel D, Solawetz W, et al (2008) A phenylalanine in DGAT is a key determinant of oil content and composition in maize. Nat Genet **40:** 367–372

Zou J, Katavic V, Giblin EM, Barton DL, MacKenzie SL, Keller WA, Hu X, Taylor DC (1997) Modification of seed oil content and acyl composition in the Brassicaceae by expression of a yeast sn-2 acyltransferase gene. Plant Cell **9:** 909–923

Zuckerkandl E, Pauling L (1965) Evolutionary divergence and convergence in proteins (vertebrate). *In* V Bryson, HJ Vogel, eds, Evolving Genes and Proteins: A Symposium Held at the Institute of Microbiology of Rutgers, The State University, 17-18 September, 1964. Academic Press, New York, pp 97–166